First publ. in: Limnology and Oceanography 47 (2002), 1, pp. 186-197

Modeling 50 years of historical temperature profiles in a large central European lake

Frank Peeters[1] *and David M. Livingstone*
Environmental Isotopes Group, Water Resources Department, Swiss Federal Institute of Environmental Science and Technology (EAWAG), Überlandstrasse 133, CH-8600 Dübendorf, Switzerland

Gerrit-Hein Goudsmit
Nordostschweizerische Kraftwerke, Abteilung FIC, Parkstrasse 23, CH-5401 Baden, Switzerland

Rolf Kipfer
Environmental Isotopes Group, Water Resources Department, Swiss Federal Institute of Environmental Science and Technology (EAWAG), Überlandstrasse 133, CH-8600 Dübendorf, Switzerland

Richard Forster
Wasserversorgung Zürich, Hardhof 9, CH-8023 Zürich, Switzerland

Abstract

A unique data set of 50 years of monthly temperature profiles from Lake Zurich, a normally ice-free lake located on the Swiss Plateau, allowed the one-dimensional numerical k-ε lake model ''SIMSTRAT'' to be calibrated (1948–1957) and validated (1958–1997). Hindcasts of temperature profiles agree excellently with the measured data. Both interannual and intraannual variations in thermal structure are reproduced well during the entire 50-yr simulation, thus demonstrating the stability and good prognostic qualities of the model. Simulations conducted with raised and lowered air temperatures (T_{air}) suggest that an increase in T_{air} will lead to an increase in lake water temperature at all depths. In comparison to the continuous modeling approach taken in this study, the commonly employed discontinuous modeling approach (with no heat carryover during winter) substantially underestimated the degree of long-term hypolimnetic warming that can be expected to result from an increase in T_{air}. Thus, whereas the discontinuous approach yields valid predictions for strictly dimictic lakes that are ice-covered each winter, heat carryover during winter makes a continuous approach necessary in lakes like Lake Zurich that are only facultatively dimictic. The significant degree of hypolimnetic warming found in this study suggests that the response of facultatively dimictic lakes to increases in T_{air} is likely to differ from that of the strictly dimictic lakes modeled in other investigations. In Lake Zurich, an increase in T_{air} is predicted to result in more frequent suppression of deeply penetrative winter mixing events, with a potentially negative impact on the lake ecosystem.

In the vast majority of lakes, the vertical temperature distribution and the intensity of vertical mixing are determined predominantly by meteorological forcing at the lake surface. A change in climatic conditions affecting this local meteorological forcing will therefore alter both thermal structure and vertical transport by mixing, which in turn will affect the flux of nutrients and dissolved oxygen, as well as the productivity and composition of the plankton (Imboden 1990; Reynolds 1997). This paper describes the long-term simulation of the thermal structure of a large temperate central European lake (Lake Zurich, Switzerland) based on meteorological data and validated using a unique 50-yr data set of measured monthly temperature profiles. We consider this as a first step toward predicting the potential effect of future climatic change on the lake ecosystem.

Previous modeling studies conducted to estimate the physical response of lakes to future climatic change (Robertson and Ragotzkie 1990; Hondzo and Stefan 1991, 1993; Huttula et al. 1992; Hostetler 1995; Elo et al. 1998; Stefan et al. 1998) have been confined to strictly dimictic lakes that freeze over each winter. In many of these studies, lake temperatures were not modeled continuously over a number of years, but instead a discontinuous approach was taken in which each year was modeled individually. This was done by setting the simulation to begin on a specific day on which the lake was assumed to be homothermic at a particular temperature, e.g., on 1 April at 4°C (Hondzo and Stefan 1991), on 1 March at 4°C (Hondzo and Stefan 1993), or 1 d after ice break-up at 3°C (Robertson and Ragotzkie 1990). Hondzo and Stefan (1993) pointed out that choosing an initial temperature profile prevents the annual carryover of heat stored in the lake during the winter period, potentially distorting the long-term results. However, continuous long-term

[1] Corresponding author (peeters@eawag.ch).

Acknowledgements

The earlier lake temperature data employed in this study (1948–1975) were measured by the Zurich Cantonal Laboratory and were kindly made available to us by the Canton of Zurich Office of Waste, Water, Energy, and Air (AWEL). The later lake temperature data (1972–1997) were measured by the City of Zurich Water Supply (WVZ). The meteorological data were made available by the Swiss Meteorological Institute. Funding was provided by the Swiss Federal Office of Education and Science (BBW; grant 97.0344) within the framework of the European Union Environment and Climate project REFLECT (Response of European Freshwater Lakes to Environmental and Climatic Change; contract ENV4-CT97-0453).

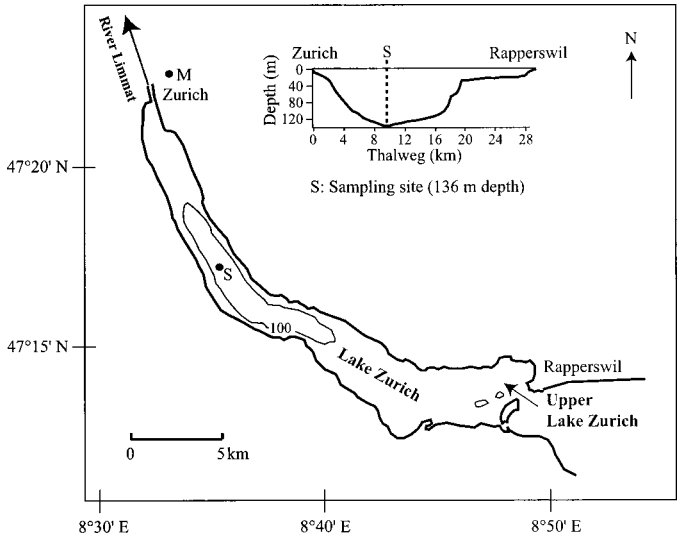

Fig. 1. Outline map of Lake Zurich. Inset: variation of lake depth along the thalweg (the line joining the deepest points of successive cross sections along the lake basin). Arrows: main inflow and outflow. M: Zurich meteorological station. Redrawn from Kutschke (1966). Temperature sampling was conducted at point *S*.

simulations of the thermal structure of lakes with annual ice cover by Stefan et al. (1998) essentially confirmed the earlier results of Hondzo and Stefan (1993), which were based on a discontinuous open-water model. The only significant difference between the two was a delay of a few days in the timing of spring overturn (Stefan et al. 1998). Conclusions drawn from the continuous modeling of the response of Finnish lakes with annual ice cover to climate change (Huttula et al. 1992; Elo et al. 1998) essentially agree with the findings of Stefan et al. (1998). Thus, a discontinuous approach neglecting the carryover of heat from year to year may be acceptable in the case of strictly dimictic lakes that freeze over each year. In the case of lakes that only rarely freeze over—i.e., facultatively dimictic temperate lakes—the thermal structure does, however, depend on the heat accumulated in the previous year and on the heat flux during winter, as will be demonstrated in this study. In such cases, a continuous approach to prognostic modeling is necessary.

In contrast to the lakes considered in these earlier modeling studies, Lake Zurich was completely ice covered only once during the second half of the 20th century (in 1963), allowing a long-term continuous simulation of its thermal structure to be conducted without requiring a sophisticated ice model. The existence of the abovementioned 50-yr data set of monthly temperature profiles allowed the reliability of the long-term simulation to be tested. To our knowledge, this paper presents the first attempt to model the thermal structure of a lake continuously over a period of as long as half a century.

Lake characteristics and data

Site—Lake Zurich is a long (30 km) narrow (2.5 km) lake situated at 406 m above sea level in the northern perialpine region of Switzerland (Fig. 1). It has a maximum depth of 136 m, a surface area of 65 km^2, and a volume of 3.3 km^3. The lake has one outflow with a mean discharge rate of 90 $m^3\ s^{-1}$, giving a mean refill time of ~420 d (Omlin et al. 2001). About 84% of the water entering the lake comes directly from the epilimnion of Upper Lake Zurich (Omlin et al. 2001), which is separated from Lake Zurich proper by a sill about 3 m deep. The large mean refill time of the lake, combined with the buffering function of Upper Lake Zurich, allows heat exchange due to throughflow to be neglected.

In Lake Zurich, stratification of the water column is dominated by temperature gradients. Conductivity data indicate that the effect of salinity gradients on density profiles can be neglected for the purpose of this study.

In the following, a distinction is made between the epi/metalimnion and the hypolimnion. Following Örn (1980), the border between the metalimnion and the hypolimnion of Lake Zurich is defined as being at 20 m.

Lake temperature data—The measurement of monthly temperature profiles in Lake Zurich began in 1936, and, with the exception of several years during World War II, has continued uninterruptedly up to the present (Kutschke 1966; Livingstone 1993, in press). The data employed here consist of 50 yr of monthly temperature profiles measured at the deepest point of the lake from 1948–1997. Typically, temperatures were measured at 0.3, 1, 2.5, 5, 7.5, 10, 12.5, 15, 20, 30, 40, 60, 80, 90, 100, 110, 120, 130, and 135 m, thus providing detailed information on the temperatures prevailing in all depth regions of the lake. All temperatures are considered to be accurate to within ± 0.1°C. The earliest (pre-1960s) temperature data were measured using a high-quality reversing thermometer (E. A. Thomas, pers. comm.), while later data were obtained by thermistor using either a Wheatstone Bridge (manually) or an automatic digital thermistor meter.

Meteorological data—The Zurich meteorological station, located within 1 km of the northern lake shore (Fig. 1), supplied data on wind speed and direction, air temperature, water vapor pressure, cloud cover, and solar radiation for this study. However, the data resolution during most of the study period was only three measurements per day. In order to take adequate account of the diel cycle in meteorological forcing, which a statistical analysis has suggested may be important for the long-term development of the thermal structure of the lake (Livingstone in press), the meteorological data were interpolated at hourly intervals. Although the coarseness of the available meteorological data might at first sight be perceived to be a disadvantage, this is not in fact the case. In order to make convincing predictions of the effects of climate change on the thermal structure of a lake, a physical lake model first has to demonstrate success in simulating the main features of the thermal structure without the luxury of accurate, high-resolution input data. Hourly air temperature estimates were determined by applying a cubic spline to the three daily observations and if necessary clipping the interpolated values to ensure that the observed daily extrema were not exceeded. Hourly estimates of wind speed, the components of the wind vector, relative humidity, cloud cover, and air pressure were calculated by simple linear inter-

polation. The hourly wind direction was defined as the direction of the hourly wind vector, determined from the estimated hourly components. The empirical equations of Gill (1982) were used to calculate hourly values of water vapor pressure from the hourly estimates of relative humidity, air temperature, and air pressure. Hourly values of solar radiation R_S were estimated from cloud cover C and clear-sky global radiation R_G using the empirical equation of Kasten and Czeplak (1980):

$$R_S = R_G(1 - a\,C^b) \tag{1}$$

Hourly values of R_G at the latitude of Lake Zurich were calculated using the approach of Brock (1981) and the atmospheric transmission coefficients of Hottel (1976). The values of the coefficients a (0.74) and b (2.9) were determined by least-squares fitting using the cloud cover observations and simultaneous measurements of solar radiation available for the Zurich meteorological station from 1982 to 1997. They lie within the range of values found by Kasten and Czeplak (1980) for Germany.

The hourly meteorological data set generated as described above was employed to drive SIMSTRAT. This model, which operates with an internal time step of 10 min, automatically performs a linear interpolation of the required meteorological variables to yield an input data set with the correct time step.

Light extinction coefficient—Because solar radiation is absorbed within the water column rather than at the air–water interface, the vertical distribution of heat depends not only on vertical mixing processes, but also on light extinction. This was modeled using a light extinction coefficient K_d assuming Beer's Law to apply (Hocking and Straškraba 1999). Values of K_d were calculated from monthly measurements of the light attenuation depth (white light) to 10%, 1%, and 0.1%, available for 1972–1997. For simplicity, vertical, seasonal, and interannual variations of K_d, which typically cover the range from 0.2 to 0.9 m^{-1}, were ignored, and the mean value of $K_d = 0.4$ m^{-1} was employed.

Model

This study employs SIMSTRAT, a slightly modified version of the one-dimensional vertical transport model for lakes and reservoirs developed by Goudsmit et al. (in press). The only driving variables required are meteorological data. In brief, a buoyancy-extended one-dimensional k-ε model (Burchard and Baumert 1995; Burchard et al. 1998) has been adapted to the specific conditions pertaining in enclosed basins by accounting for the variable cross-section as a function of depth and by including a simplified seiche model. The relevant governing equations included in SIMSTRAT are listed in Table 1. In a k-ε model, vertical turbulent diffusivities ν_t' are determined from the turbulent kinetic energy k and energy dissipation ε. ν_t' determines the vertical diffusive transport of dissolved substances and heat. In the absence of water inflow and outflow, the temperature distribution can be calculated from the heat fluxes at the lake boundaries using ν_t'.

Table 1. Governing equations of the k-ε model and extensions included in SIMSTRAT (Goudsmit et al. in press).

$$\frac{\partial T}{\partial t} = \frac{1}{A}\frac{\partial}{\partial z}\left(A(\nu_t' + \nu')\frac{\partial T}{\partial z}\right) + \frac{1}{\rho_0 c_p}\frac{\partial H_{\text{sol}}}{\partial z} + \frac{\partial A}{\partial z}\frac{H_{\text{geo}}}{A\rho_0 c_p}$$

$$\frac{\partial U}{\partial t} = \frac{1}{A}\frac{\partial}{\partial z}\left(A(\nu_t + \nu)\frac{\partial U}{\partial z}\right) + fV$$

$$\frac{\partial V}{\partial t} = \frac{1}{A}\frac{\partial}{\partial z}\left(A(\nu_t + \nu)\frac{\partial V}{\partial z}\right) - fU$$

$$\frac{\partial k}{\partial t} = \frac{1}{A}\frac{\partial}{\partial z}\left(A\nu_k\frac{\partial k}{\partial z}\right) + P + P_{\text{seiche}} + B - \varepsilon$$

$$\frac{\partial \varepsilon}{\partial t} = \frac{1}{A}\frac{\partial}{\partial z}\left(A\nu_\varepsilon\frac{\partial \varepsilon}{\partial z}\right) + \frac{\varepsilon}{k}(c_{\varepsilon 1}(P + P_{\text{seiche}}) + c_{\varepsilon 3}B - c_{\varepsilon 2}\varepsilon)$$

$$P = \nu_t\left(\left(\frac{\partial U}{\partial z}\right)^2 + \left(\frac{\partial V}{\partial z}\right)^2\right) \qquad B = -\nu_t' N^2$$

$$\nu_t = c_\mu\frac{k^2}{\varepsilon} \qquad \nu_t' = c_\mu'\frac{k^2}{\varepsilon}$$

$$\nu_k = \frac{c_\mu}{\sigma_k}\frac{k^2}{\varepsilon} \qquad \nu_\varepsilon = \frac{c_\mu}{\sigma_\varepsilon}\frac{k^2}{\varepsilon}$$

Definitions:

T	temperature (°C)
U	horizontal velocity west–east (m s^{-1})
V	horizontal velocity south–north (m s^{-1})
k	turbulent kinetic energy per unit mass (J kg^{-1})
ε	dissipation rate of k (W kg^{-1})
ν	molecular viscosity, 1.5×10^{-6} m^2 s^{-1}
ν'	molecular diffusivity, 1.5×10^{-7} m^2 s^{-1}
ν_t	turbulent viscosity (m^2 s^{-1})
ν_t'	turbulent diffusivity (m^2 s^{-1})
ν_ε	turbulent diffusivity of ε (m^2 s^{-1})
ν_k	turbulent diffusivity of k (m^2 s^{-1})
B	buoyancy flux (W kg^{-1})
P	production of k due to shear stress (W kg^{-1})
P_{seiche}	production of k due to internal seiching (W kg^{-1})
t	time (s)
z	depth (positive upward) (m)
A	cross-sectional area at z (m^2)
f	Coriolis parameter (s^{-1})
c_p	specific heat of lake water (J kg^{-1} K^{-1})
ρ_0	density of lake water (kg m^{-3})
H_{sol}	short-wave solar radiation at z (W m^{-2})
H_{geo}	geothermal heat flux (W m^{-2})
N^2	Brunt-Väisälä frequency (s^{-1})

Constants of the k-ε model:

$c_{\varepsilon 1}$	1.44
$c_{\varepsilon 2}$	1.92
$c_{\varepsilon 3}$	−0.4 if $B < 0$ else 1
c_μ	0.09
c_μ'	0.072
σ_k	1.00
σ_ε	1.3

Model description—In SIMSTRAT, turbulent kinetic energy k is generated by current shear due to wind forcing and by convection due to heat loss at the lake surface. If stratification is negative, the buoyancy flux is positive (i.e., potential energy decreases during the mixing process), which results in increased turbulent kinetic energy and increased diffusivity (Table 1). Hence, SIMSTRAT models mixing due to convection as a diffusive process. The main sink of turbulent

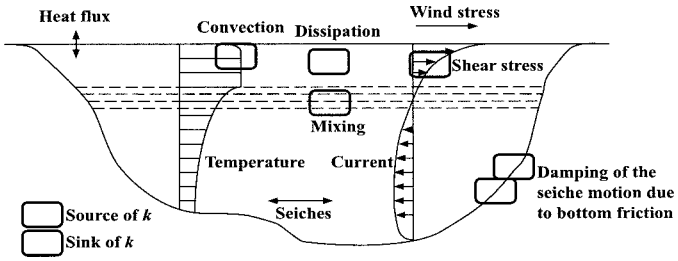

Fig. 2. Schematic diagram of the processes taken account of by the one-dimensional physical lake model SIMSTRAT in modeling Lake Zurich.

kinetic energy is energy dissipation. If the water column is stably stratified, mixing results in an increase in potential energy. In this case the buoyancy flux is negative and acts as a sink of turbulent kinetic energy (Fig. 2).

Kinetic energy, which is introduced directly at the lake surface by wind forcing, decreases rapidly with depth. In the deep water below the thermocline, the main source of turbulent kinetic energy is seiche motion. This source of k is accounted for by a simplified seiche model that assumes that a fixed proportion (α) of the wind power acting at the lake surface flows directly into the seiche motion and that the seiche energy decays by friction at the bottom boundaries, assuming law-of-the-wall behavior:

$$\frac{dE_{\text{seiche}}}{dt} = PW - LS$$

with

$$PW = \alpha\, A_0\, \rho_{\text{air}}\, C_{10}\, (u_{10}^2 + v_{10}^2)^{3/2} \quad \text{and}$$

$$LS = A_0\, V_0^{-3/2} \rho_0^{-1/2}\, C_{\text{eff}}\, E_{\text{seiche}}^{3/2} \tag{2}$$

where E_{seiche} is the mean kinetic energy of the seiching and PW and LS are the rates of production and loss, respectively, of seiche energy. A_0 is the lake surface area, V_0 the lake volume, ρ_{air} the density of air, ρ_0 the density of water, u_{10} and v_{10} the horizontal components of the wind vector 10 m above the lake surface, C_{10} the drag coefficient 10 m above the lake surface and C_{eff} the effective bottom drag coefficient. The functional form of LS is adapted from the seiche damping model of Gloor et al. (2000).

The seiche energy is lost to the production of turbulent kinetic energy $P_{\text{seiche,tot}}$ and to the generation of heat in the viscous sublayer. Thus $P_{\text{seiche,tot}} = \text{LS} - \text{LS}\, 10\sqrt{C_{\text{eff}}}$, where the second term describes the kinetic energy dissipation in the viscous sublayer (Imboden and Wüest 1995). The production of k from the seiche motion is assumed to be accompanied by a production of ε that is modeled analogously to the production of ε from current shear.

To obtain the vertical distribution of the production of turbulent kinetic energy $P_{\text{seiche}}(z)$ due to seiching, we assume that the energy loss from the seiche motion is proportional to the sediment area and is a function of the stability N^2 of the water column (where N is the Brunt-Väisälä frequency). The justification for these assumptions is the fact that bottom friction is the dominant cause of the loss of seiche energy, and the fact that the vertical velocity shear can be expected to be largest at those depths where the stability is highest. Combining the different assumptions, and using the fact that the total sediment area is approximately equal to the lake surface area, leads to the following empirical equation for the generation of turbulent kinetic energy from the seiche energy (Goudsmit et al. in press):

$$\begin{aligned} P_{\text{seiche}}(z) &= c_{\text{norm}}\, N^{2q}\, \frac{LS}{A_0}\, (1 - 10\sqrt{C_{\text{eff}}})\, \frac{1}{A}\, \frac{dA}{dz} \\ &= c_{\text{norm}}\, N^{2q}\, C_{\text{eff}}\, V_0^{-3/2} \rho_0^{-1/2}\, E_{\text{seiche}}^{3/2}\, (1 - 10\sqrt{C_{\text{eff}}}) \\ &\quad \times \frac{1}{A}\, \frac{dA}{dz} \end{aligned} \tag{3a}$$

with

$$c_{\text{norm}} = \left(\int_{z_{\text{bottom}}}^{z_{\text{surface}}} N(z')^{2q}\, \frac{dA(z')}{dz'}\, dz' \right)^{-1} \tag{3b}$$

where A is the isobath area at depth z, q is an empirical parameter, and the normalization (Eq. 3b) assures that the integration of $P_{\text{seiche}}(z)$ over the entire water column gives the total production of k by the seiche motion, $P_{\text{seiche,tot}}$.

The parameters α, C_{eff}, and q in Eq. 3 are lake-specific. They are the only parameters of the lake model related to internal transport that require adjustment by model calibration.

Boundary conditions, model parameters, and numerical implementation—At the bottom boundaries, velocity is assumed to decrease due to bottom friction with a friction coefficient $C_{\text{bottom}} = 1.5 \times 10^{-3}$ (Elliott 1984). At the top and bottom boundaries we assume no flux of k and use a flux boundary condition for ε (Goudsmit et al. in press). In the calculation of the temperature profiles we include a geothermal heat flux of 0.1 W m^{-2} (Finckh 1981) through the bottom boundaries as a source term. The heat fluxes through the lake surface are described by the empirical relationships summarized by Livingstone and Imboden (1989), based on Edinger et al. (1968). Following Kuhn (1977, 1978) and Livingstone and Imboden (1989), the model includes two calibration parameters, p_1 and p_2, which allow adjustment of the empirical relationships describing (1) the heat flux due to incoming atmospheric long-wave radiation and (2) the wind function used in the calculation of the fluxes of latent and sensible heat. Finally, we also treat the wind friction coefficient C_{10} as an adjustable parameter. The calibration parameters p_1, p_2, and C_{10} may implicitly take into account the fact that available meteorological data for lake modeling studies are usually measured some distance from the lake. In total, therefore, the model allows the adjustment of only six calibration parameters (α, q, C_{eff}, C_{10}, p_1, and p_2), all of which were assumed to be time-invariant in this study.

The current version of SIMSTRAT does not include a sophisticated ice model and therefore cannot adequately describe either the heat fluxes through the ice and snow cover or the duration of ice cover. To prevent the lake surface water cooling to values significantly below 0°C, the net heat flux is set to zero if the net heat flux determined using the em-

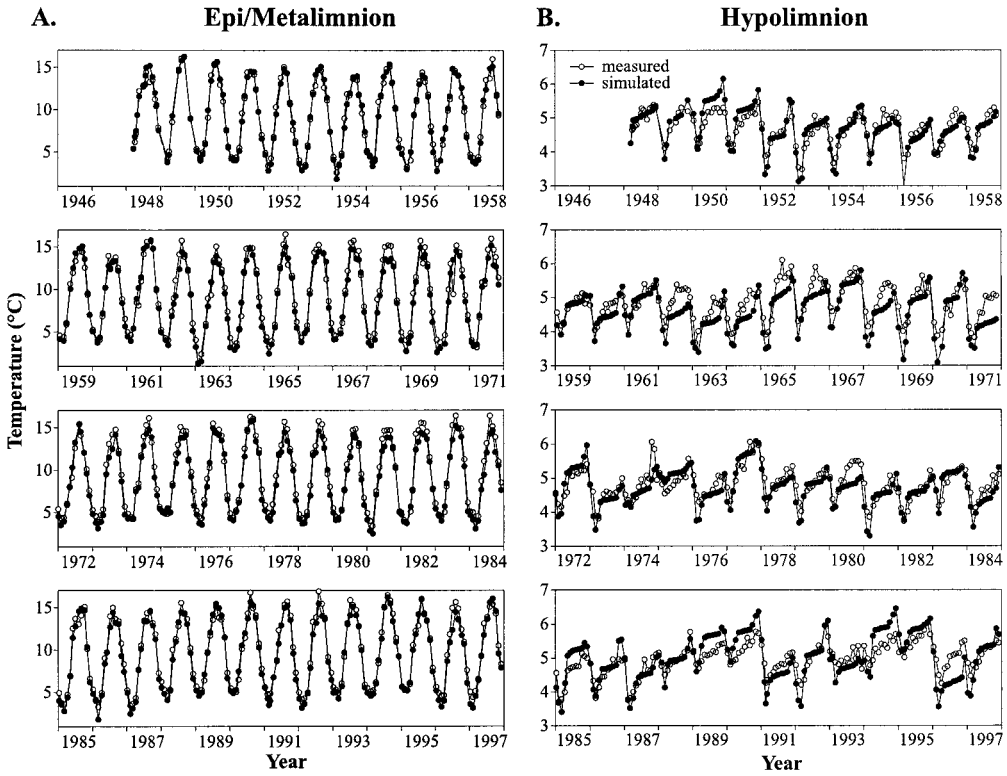

Fig. 3. Comparison of volume-weighted mean temperatures derived from measured data and simulations. Volume-weighted mean temperature of (A) the epi/metalimnion (T_{em}, 0–20 m) and (B) the hypolimnion (T_h, 20–136 m).

pirical relationships for open water is negative and the surface water temperature is below 0°C.

The differential equations describing the transport model are solved numerically using the method of lines and an implicit double-sweep algorithm. The FORTRAN code of SIMSTRAT uses the numerical scheme of Burchard and Baumert (1995). Details on the numerical implementation of the model are given by Goudsmit et al. (in press). For the present study a slight modification of the model was made by altering the grid structure for k and ε for the uppermost and lowermost grid points.

Throughout this study we use an internal time step of 10 min and a total of 500 grid points, providing a vertical resolution of better than 30 cm. The initial values for the temperature were always taken from an observed temperature profile.

Calibration of the six adjustable model parameters by least-squares fitting was based on the first 10 yr of the data set (1948–1957), leaving the 40-yr time period from 1958 to 1997 for model validation. The following values were obtained: $\alpha = 5.3 \times 10^{-3}$, $q = 1$, $C_{\text{eff}} = 1.2 \times 10^{-3}$, $C_{10} = 1.3 \times 10^{-3}$, $p_1 = 1.24$, and $p_2 = 1.26$. These parameter values obtained from the 1948–1957 calibration period were employed in all simulations presented here. Model runs covering time periods after 1957 can therefore be considered as prognostic simulations.

Results

Long-term simulation of historical lake thermal structure—SIMSTRAT was employed to provide a continuous simulation of the thermal structure of the lake from 1948 to 1997. Note that SIMSTRAT is extremely stable, so that it was not necessary to tie the simulated temperatures to measured values at any time during the model run (except for one initial profile in March 1948). The simulated heat content of Lake Zurich agrees excellently with observed values over the entire 50-yr time period. The mean difference between observed and predicted heat content, expressed as the volume-weighted mean lake temperature T_1, is only 0.18°C ± 0.37°C, and the root mean square difference (RMSD) is only 0.42°C. A comparison of simulated and measured values of the volume-weighted mean temperatures of the epi/metalimnion (T_{em}, 0–20 m, Fig. 3A) and hypolimnion (T_h, 20–136 m, Fig. 3B) shows that these are also represented very well by the model. The mean differences between simulated and measured values are 0.37°C ± 0.67°C (T_{em}) and 0.08°C ± 0.34°C (T_h); the corresponding RMSDs are 0.77°C and 0.34°C, respectively.

The model generally underestimates the mean temperature of the hypolimnion slightly in spring, and in some years also in summer. However, in most years the predicted seasonal variation in T_h agrees well with the observed data. Note that

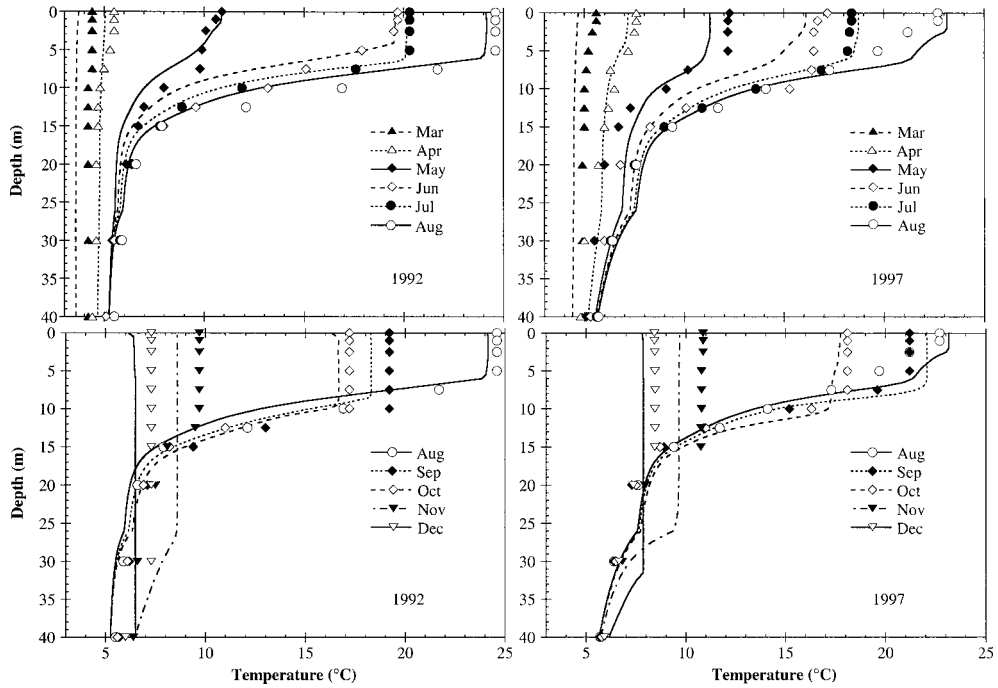

Fig. 4. Comparison of simulated temperature profiles (lines) with measured data (symbols) during periods of stratification (upper panels) and destratification (lower panels). Shown are the years 1992 and 1997, which correspond to model predictions after simulation periods of 45 yr and 50 yr, respectively. Simulations were started in March 1948.

the ''sawtooth'' structure of the climate-induced temporal change in T_h that occurred between 1987 and 1991 as a result of three consecutive warm winters, as described by Livingstone (1993, 1997) (a gradual increase over several years followed by an abrupt decrease), is represented well by the model (Fig. 3B). The model predicts a similar ''sawtooth'' structure for the time period 1992–1996, which is confirmed by the data.

Simulated seasonal variations and details of the vertical temperature distribution agree very well with the corresponding observations, even if the simulation covers very long time periods. Figure 4 compares simulated temperature profiles (lines) with measured profiles (symbols) for the stratification and destratification periods in two representative years near the end of the simulation, viz. 1992 and 1997. Note that the simulation was started in January 1948, so the predicted profiles represent the results of modeling periods of 45 yr and 50 yr, respectively. Figure 4 demonstrates not only that the seasonal variability in the profiles is captured well by the model, but also that both the timing of the onset of stratification and the depth of the thermocline are also reproduced well. The only significant discrepancy between measured and simulated temperatures is an overestimate of the degree of vertical mixing in November.

The mean difference between all observed temperatures (11,267 samples) and the corresponding simulated temperatures is 0.18°C ± 0.83°C, indicating a slight overall underestimate. The RMSD between all data and model prediction is 0.84°C. This value is dominated by contributions from the metalimnion in summer, because a small error in the modeled depth of the summer thermocline leads to a large deviation between simulated and observed temperatures within the metalimnion, where temperature gradients are steep.

Simulated daily mean lake surface temperatures (T_0) between 1948 and 1997 reveal a high degree of interannual variation, both in summer and in winter. Summer maxima range from 21.6°C to 26.5°C and winter minima from 0.0°C to 4.8°C. In 33 of the 49 winters, simulated values of T_0 always exceed 2°C, and in 24 of these, the simulated minimum temperature is above 3°C. However, SIMSTRAT predicts an exceptionally long time period of 0°C surface water temperatures between January and March in 1963, the only year during the time period covered by the simulation when Lake Zurich was completely frozen over, viz. from 23 January to 27 March (Lemans 1964).

Sensitivity analysis with respect to air temperature—The model results essentially depend on five meteorological variables; viz. air temperature, wind speed, wind direction, water vapor pressure, and cloud cover. One of the most important predictions concerning the development of the global climate during the 21st century is that at least one of these variables, viz. air temperature, will change significantly (Kattenberg et al. 1996). Compared to air temperature, the likely future development of the other four driving variables is still unclear both globally and regionally, making it difficult or impossible to make concrete predictions of the future development of lake thermal structure. However, of all meteorological driving variables, air temperature (T_{air}) is considered to have the most significant effect on lake temperature variability (Henderson-Sellers 1988; Hondzo and Stefan 1992, 1993). Therefore, even if no concrete predic-

tions can be made, the use of SIMSTRAT as a tool to perform a sensitivity analysis of lake temperature with respect to air temperature alone can still yield information that may contribute to an understanding of what may happen to the thermal structure of lakes in a warmer world.

To estimate the potential effect of changing air temperatures (T_{air}) on the thermal structure of the lake, the model was rerun under the same conditions starting in 1948 and using the same meteorological data as above, but with T_{air} raised or lowered by a certain constant amount with respect to the original values. This approach can be interpreted as a sensitivity analysis with respect to T_{air}. The maximum increase in T_{air} considered in this investigation is 4°C, i.e., 0.5°C less than the maximum global annual mean warming predicted for 2100 by IPCC scenario IS92e with high climate sensitivity (Kattenberg et al. 1996). Earlier investigations studying the effect of climate warming on thermal stratification in lakes have assumed a similar magnitude for the shift in T_{air}: Robertson and Ragotzkie (1990) considered shifts of between −3°C and +5°C, Huttula et al. (1992) used climate scenarios predicting an annual mean shift of about +4°C, and the scenarios employed by Hondzo and Stefan (1993) and Stefan et al. (1998) predict an annual mean shift of about 5°C.

Figure 5 shows the effect on T_{em} and T_h during 1985–1997 of raising and lowering T_{air} by 4°C. Higher (lower) T_{air} results in increased (decreased) water temperatures in all years and during all seasons. Note that the magnitude of the shift in T_{em} is about the same for raised and lowered T_{air}, while the magnitude of the shift in T_h is greater for raised than for lowered T_{air}. For raised T_{air}, the sawtooth structure occurring in T_h between 1987 and 1991 is more pronounced than for lowered T_{air}, and convective cooling of the hypolimnion in early spring appears to be much weaker than under present conditions (Fig. 5B). On average, a shift in T_{air} of +4°C (−4°C) results in a shift of +1.9°C (−1.6°C) in T_{em} and +1.4°C (−0.7°C) in T_h (Fig. 6A). Thus, a general 4°C rise in T_{air} is predicted to increase the temperature difference ($T_{em} - T_h$) between the epi/metalimnion and the hypolimnion by an average of 0.5°C (Fig. 6B, solid triangles), resulting in an increase in thermal stability, whereas a lowering of T_{air} by the same amount is predicted to reduce ($T_{em} - T_h$) by an average of 0.9°C (Fig. 6B, open circles), resulting in a decrease in thermal stability.

Figure 7 demonstrates how strongly different changes in T_{air} are predicted to affect mean temperatures at various depths in the lake. The mean lake surface temperature (T_0) is predicted to increase linearly with increasing T_{air} at a rate $dT_0/dT_{air} = 0.55$. Temperatures within the water column (T_z) are predicted to be affected more strongly by increasing T_{air} than by decreasing T_{air}; i.e., dT_z/dT_{air} increases with increasing T_{air}. Shifts in mean water temperatures are predicted to be stronger in the epi/metalimnion than in the hypolimnion. An increase in T_{air} is predicted to have a greater effect on the difference between T_{em} and T_h, and between T_0 and T_{100}, than a decrease in T_{air} (Fig. 7B).

Comparison of continuous and discontinuous modeling approaches—The seasonal effect of increased T_{air} on water temperatures and the importance of employing the continuous as opposed to the discontinuous approach to modeling the response of lake thermal structure to climatic forcing is demonstrated in Fig. 8. Figure 8 shows the predicted change in the monthly means of T_{em}, T_h, and $T_{em} - T_h$ assuming ambient T_{air} to be 4°C higher than today. The predicted effect on these monthly mean lake temperatures of raising T_{air} can be seen to depend strongly on whether a continuous approach (Fig. 8A,C,E) or discontinuous approach (Figs. 8B,D,F) is employed.

Continuous model runs were conducted starting from the temperature profile measured in March 1948 and predicting water temperatures for the 50-yr time period up to 1997. This approach predicts raised T_{air} to result in higher water temperatures at all depths and in all months, including March. Temperatures in the hypolimnion (Fig. 8C) increase more strongly following a warm winter (e.g., 1989, circles) than after a cold winter (e.g., 1987, open triangles). Solid

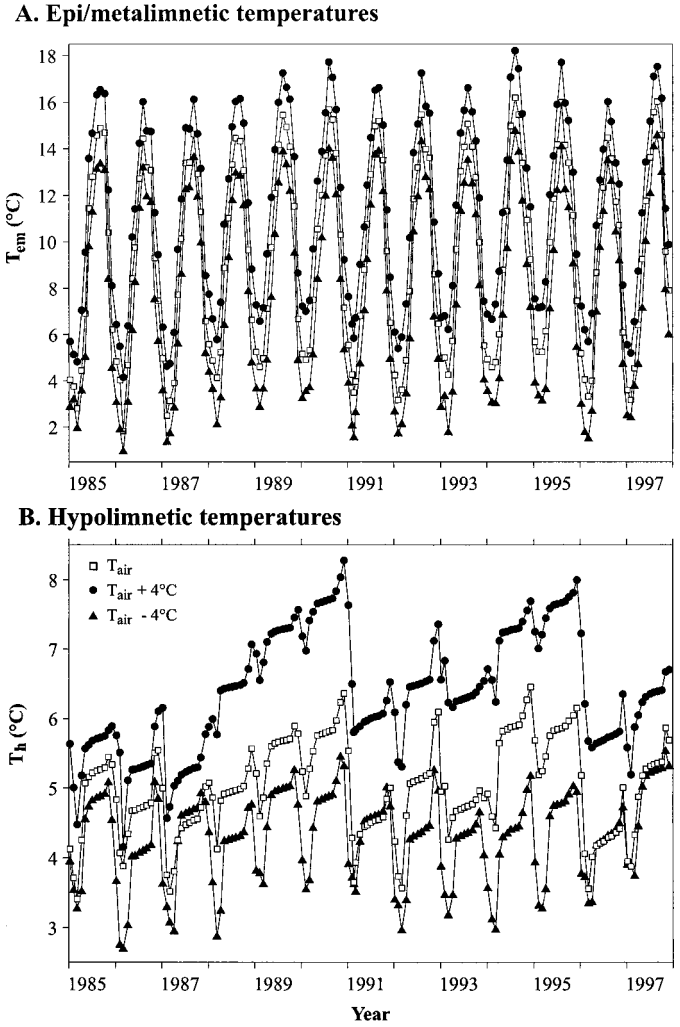

Fig. 5. Comparison of model results for (A) epi/metalimnetic temperatures T_{em} and (B) hypolimnetic temperatures T_h obtained with the measured air temperatures (open squares) and with air temperatures shifted by +4°C (solid circles) and by −4°C (solid triangles). All simulations were started in March 1948.

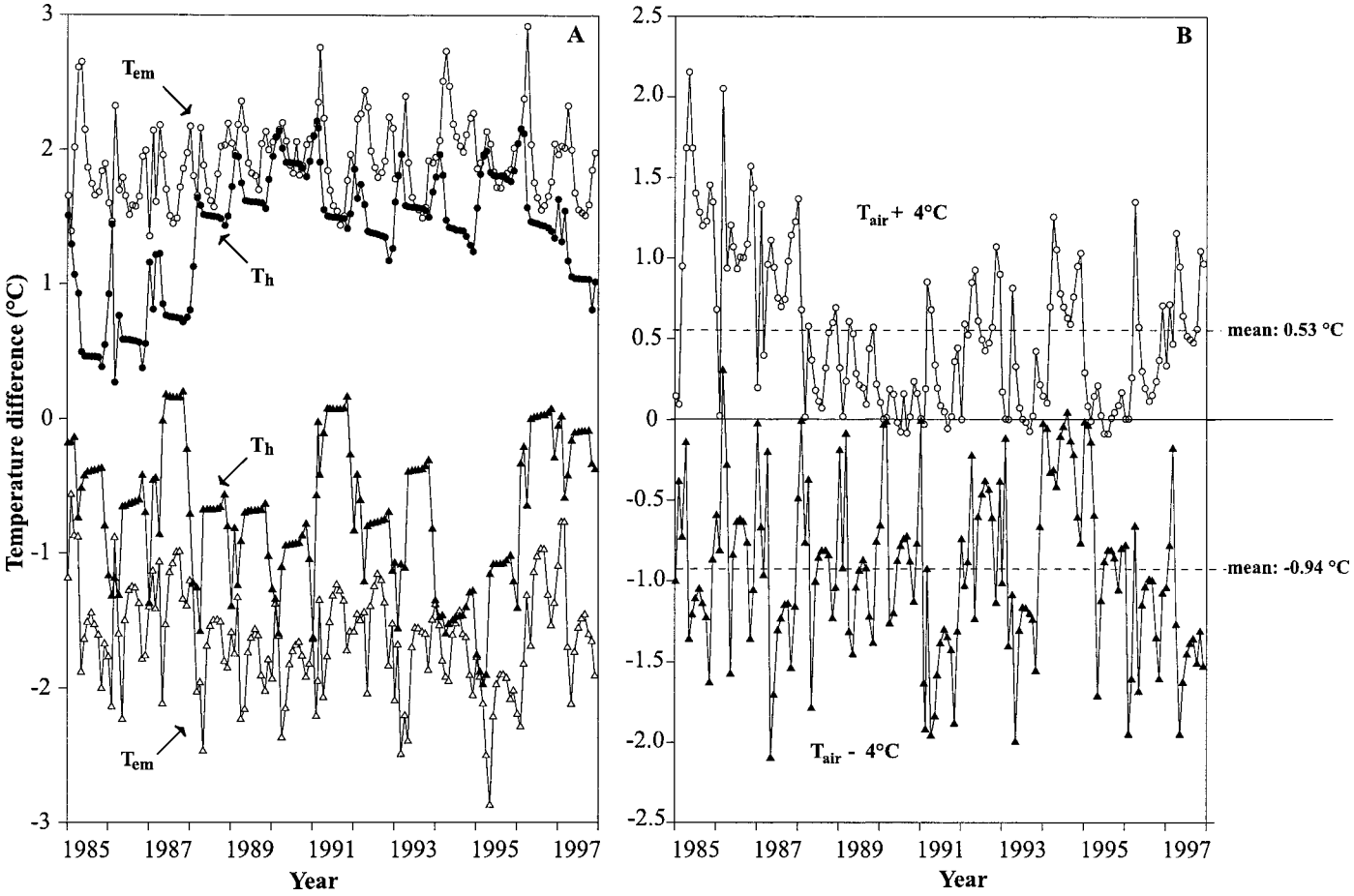

Fig. 6. Effect of ±4°C shifts in air temperature on lake temperatures. (A) Difference between simulations based on altered air temperatures and simulations based on the original air temperatures for T_{em} (open symbols) and T_h (solid symbols). Circles represent results based on simulations with air temperatures raised by 4°C, triangles those based on air temperatures lowered by 4°C. (B) The corresponding shifts in the difference ($T_{em} - T_h$). All simulations were started in March 1948.

triangles in Fig. 8 characterize the mean change in monthly mean temperatures for the period 1985–1997.

Discontinuous model runs for individual years were conducted starting from the temperature profile measured during spring circulation in March of the year of interest and predicting water temperatures for the rest of the year. Predictions based on the discontinuous approach differ from the above results in that they assume that an increase in T_{air} has a negligible effect on water temperatures in March. After May, the effect of raised T_{air} on surface temperatures (not shown) is about the same regardless of the model approach taken. However, with increasing depth in the water column, the discrepancy between the two approaches widens. In the epilimnion, the discontinuous approach suggests that the shift of T_{em} toward warmer temperatures is slight in spring and increases over summer and fall (Fig. 8B), while the continuous simulation indicates a similar increase in T_{em} in all seasons (Fig. 8A). Only in late fall do the discontinuous and continuous approaches predict roughly similar values of T_{em}. In the hypolimnion, the discontinuous approach leads to predictions that T_h will increase only slightly or will even decrease (Fig. 8D), rather than increasing significantly, as predicted by the continuous approach (Fig. 8C). In general, the discontinuous modeling approach predicts that an increase in T_{air} leads to a stronger change in stratification with stronger seasonal variability than that suggested by the continuous modeling approach, whereas the latter predicts much more hypolimnetic warming.

Discussion

Figures 3 and 4 indicate that the continuous model SIMSTRAT described here is able to simulate the thermal structure of Lake Zurich over a 50-yr time period with no significant drift in heat content. Calibration over a 10-yr time period is apparently sufficient to avoid a long-term drift in heat exchange. The heat exchange mechanisms at the water surface act as a self-regulating feedback system that automatically tends toward a balance corresponding to the correct heat content. If the heat flux into the lake is overestimated by the empirical equations, the simulated surface water temperature increases, resulting in an increase in the emission of long-wave radiation from the lake surface. As a consequence, the net heat flux into the lake is reduced, which leads to a reduction in the surface temperature. Note that the surface temperature also affects the fluxes of sensible and

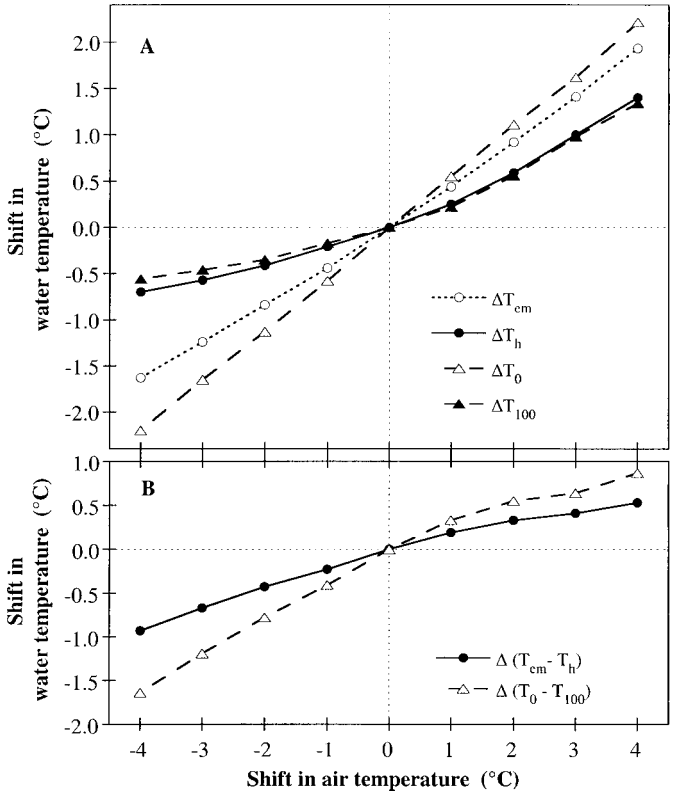

Fig. 7. The shift in water temperature associated with shifts in air temperature of −4°C to +4°C. Shown is the mean difference Δ between model predictions using altered air temperatures and predictions obtained with the original air temperatures for the period 1985–1997. Simulations were started in March 1948. (A) Shift in water temperature at the surface (ΔT_0, open triangles), at 100 m depth (ΔT_{100}, solid triangles), in the epi/metalimnion (ΔT_{em}, open circles) and the hypolimnion (ΔT_h, solid circles). (B) Shift in the temperature differences $\Delta(T_0 - T_{100})$ (triangles) and $\Delta(T_{em} - T_h)$ (circles), indicating the effect of raised/lowered air temperatures on the thermal stratification.

latent heat across the air–water interface in such a way that the feedback system is further reinforced. Because of this heat exchange feedback system and the occurrence of vigorous mixing in early spring, model predictions tend to recover after individual years of below-average performance.

Simulated and observed summer thermocline depths agree to within a few meters (Fig. 4). A better agreement between data and model predictions cannot be expected because the depth of the thermocline in the measured profile is affected by the reversible vertical motion at the sampling location due to seiching. Note that the horizontal mean of the vertical displacement due to pure seiche motion is zero, and so our one-dimensional model describing horizontal mean characteristics cannot represent the local reversible displacement of the seiche motion, but can only include the effect of the seiching on vertical mixing.

Most of the simulated time period is beyond the calibration period, so the agreement between measured and simulated temperatures indicates that the model has good prognostic qualities. The simulation period covers a variety of meteorological conditions, with January mean T_{air} ranging from −6.2°C to 3.8°C, July mean T_{air} ranging from 15.1°C to 22.3°C, and annual mean T_{air} ranging from 7.3°C to 10.4°C. This high degree of variability is reflected in the model results: simulated annual maximum surface temperatures, for instance, vary by up to 5°C between years.

SIMSTRAT is also capable of adequately simulating thermal conditions occurring during periods with exceptional climatic conditions. This is demonstrated by the successful prediction of the continuous increase in annual minimum deep-water temperatures from 1987 to 1990 and from 1992 to 1995, and the subsequent strong cooling in the winters of 1991 and 1996. The sawtooth deep-water warming/cooling episode from 1987 to 1991 is a large-scale phenomenon that occurred simultaneously in several Swiss lakes, e.g., Lake Zurich, Lake Neuchâtel, and to a lesser extent Lake Geneva and Lake Zug (Livingstone 1993, 1997). This phenomenon was caused by the exceptionally warm winters that occurred in the 3 yr preceding 1991, which resulted in exceptionally warm deep water with comparatively low density. Cooling of the surface water in early spring 1991 resulted in deep, penetrative convective mixing because of the low density of the deep water. The sawtooth episode lasting from 1992 to 1996 is probably the result of climatic conditions similar to those existing between 1987 and 1991, and both are most likely linked ultimately to the behavior of the North Atlantic Oscillation (NAO), which governs winter T_{air} in much of northern and central Europe (Hurrell 1995) and is known to leave a strong signal in lake temperatures there (Gerten and Adrian 2001; Livingstone and Dokulil 2001).

Another example demonstrating SIMSTRAT's ability to simulate the effects of extreme climatic conditions is given by early spring 1963, for which the model predicts an exceptionally long period of low water temperatures at the surface and also throughout the epi/metalimnion (Fig. 3A). Spring 1963 is the only time period in the 50 yr covered by the simulations when Lake Zurich was completely ice covered. Note that the exceptional meteorological conditions in 1963 were this time associated with an extreme reversal of the NAO (Moses et al. 1987).

The sensitivity analysis with respect to T_{air} suggests that, all else being equal, an increase of 4°C in T_{air} will lead on average to an increase of 1.9°C in T_{em} (Fig. 6B), i.e., about 50% of the increase in T_{air}. The temperature T_0 at the lake surface increases linearly with T_{air} at a rate of $dT_0/dT_{air} = 0.55$ (Fig. 7). Other studies (Robertson and Ragotzkie 1990; Hondzo and Stefan 1991, 1993; Huttula et al. 1992; Hostetler 1995; Stefan et al. 1998) also report a strong increase in T_0 with T_{air}. These earlier studies found that the effect of climatic warming on the surface water temperature is greater in summer than in winter and early spring. In contrast, the results for Lake Zurich suggest that for raised T_{air}, changes in T_0 and T_{em} are similar during all seasons (Fig. 8).

The most prominent difference with respect to the earlier investigations is the effect of enhanced T_{air} on deep-water temperatures. The earlier studies suggested that hypolimnetic temperatures should increase only very slightly or even decrease in a warmer climate (Robertson and Ragotzkie 1990; Hondzo and Stefan 1991, 1993; Huttula et al. 1992; Hostetler 1995; Stefan et al. 1998). Our simulations of the temperature distribution in Lake Zurich suggest that a 4°C in-

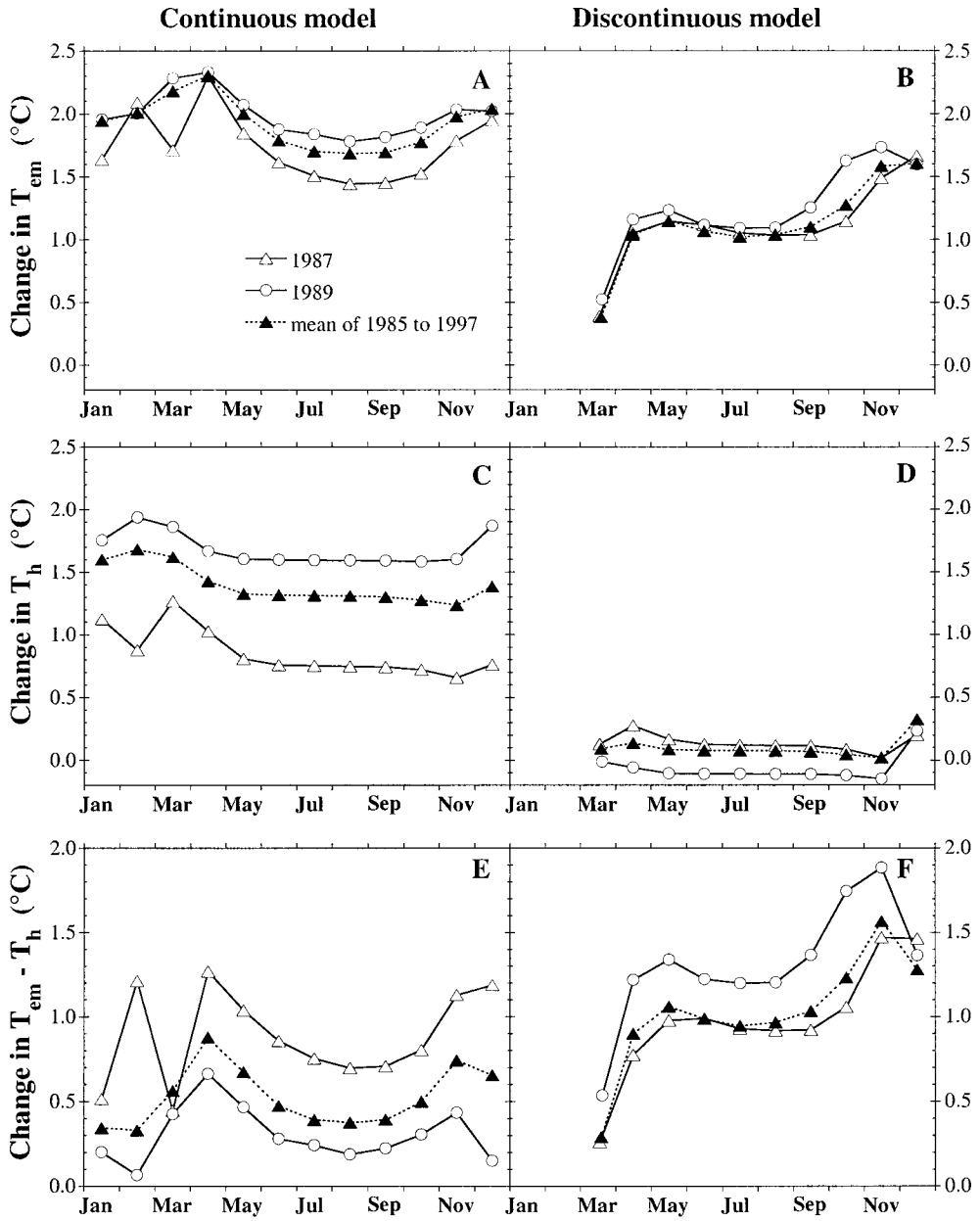

Fig. 8. Comparison of the response of lake temperature to an air temperature raised by 4°C as predicted by continuous modeling (A, C, E) and by discontinuous modeling (B, D, F). Shown is the change in mean monthly water temperature in the epi/metalimnion T_{em} (A, B), the hypolimnion T_h (C, D), and the temperature difference ($T_{em} - T_h$) (E, F) caused by raised air temperatures. Mean monthly temperature profiles were determined from temperature profiles simulated at 10-min intervals. Shown are mean values for a year after a winter with warm water temperatures (1989, open circles), for a year after a winter with cold water temperatures (1987, open triangles) and for the time period from 1985 to 1997 (solid triangles).

crease in T_{air} leads on average to an increase of about 1.4°C in T_h, which is almost as much as the increase predicted for T_{em}. As in the epilimnion, increased T_{air} leads to an increase in hypolimnetic temperatures in all seasons (Fig. 8). Apparently, in facultatively dimictic lakes such as Lake Zurich, the thermal stratification, parameterized in terms of the difference ($T_{em} - T_h$) between epi/metalimnetic and hypolimnetic water temperatures, is affected much less by a change in T_{air} (Fig. 6B, Fig. 7) than is the stratification in the strictly dimictic lakes considered in the earlier studies.

Figure 7B suggests that the thermal stratification of a lake responds asymmetrically to air temperature variations. From a physical point of view it is not the current T_{air}, but the short-term history of the water temperature of the lake, that determines how strongly the stratification responds to changes in air temperature.

Under present-day climatic conditions, surface water temperatures in Lake Zurich are around 4°C during winter and decrease to temperatures below 3°C only in 50% of the 50 years considered here. Convective mixing occurring between early winter and early spring results in deep-water temperatures close to 4°C. If T_{air} increases substantially, surface water temperatures will be above 4°C all year round, implying that Lake Zurich will shift from a facultatively dimictic to a facultatively monomictic lake. As a consequence, complete mixing, if it occurs at all, will occur only during the coldest part of the year, resulting in deep-water temperatures close to the annual minimum epilimnetic temperature, which will be above 4°C. In this case, hypolimnetic temperatures will increase in parallel to the increase in the annual minimum epilimnetic temperature. If T_{air} decreases substantially, Lake Zurich will as a rule behave dimictically, resulting in deep-water temperatures of around 4°C. In accordance with this reasoning, the hypolimnetic temperature is seen to increase much more strongly in response to raised T_{air} in years with high hypolimnetic temperatures in winter (e.g., 1989) than in years with low hypolimnetic temperatures in winter (e.g., 1987) (Fig. 8C).

A climate-induced shift from facultative dimixis to facultative monomixis can have severe ecological consequences because thermal stratification and deep-water mixing become much more susceptible to interannual variations in meteorological conditions. This is demonstrated by the sawtooth structure of T_h from 1987 to 1991. Because of reduced mixing during this time period, mean oxygen levels below 100 m in Lake Zurich dropped from 7.7 g O_2 m^{-3} to 0.7 g O_2 m^{-3} (Livingstone 1997). Although a slight increase in deep-water oxygen levels was observed each year in early spring, mixing was not sufficient to result in a recovery of sufficient magnitude to prevent the long-term decrease of dissolved oxygen caused by oxygen depletion during summer and fall. Deep-water mixing will be even further reduced during a series of warm winters if T_{air} is generally higher, as indicated in Fig. 5B. Consequently, the recovery of deep-water oxygen concentrations during winter and early spring will be much less pronounced, and the long-term decrease in oxygen levels much more rapid than observed under present climate conditions. This is likely to lead to deep-water anoxia (Livingstone and Imboden 1996), which could trigger a feedback system in which ions are released from the anoxic sediments, resulting in an increase of the chemical stability of the deep water and a consequent reduction in vertical mixing and deep-water ventilation. In meromictic Lake Zug (maximum depth 197 m), 20 km from Lake Zurich, the climate-induced reduction of deep-water mixing that occurred between 1988 and 1990 resulted in an upward shift of the 0.5 g O_2 m^{-3} isopleth by about 70 m between 1987 and 1990. A further reduction in deep-water mixing during such a series of warm winters, as must be expected to occur more frequently in the transition to a warmer climate, is likely to lead to a very critical situation for the Lake Zug ecosystem.

Continuous simulation of the thermal stratification of Lake Zurich suggests that an increase in T_{air} will lead to a temperature increase in both epilimnion and hypolimnion that is similar in all seasons (Fig. 8A,C). In contrast, predictions from discontinuous model runs for Lake Zurich, assuming a prescribed profile in March of each individual year that reflect conditions during spring circulation, suggest that an increase in T_{air} will have hardly any affect on hypolimnetic temperatures, but will cause a significant seasonally dependent temperature increase in the uppermost 20 m of the lake (Fig. 8B,D). This demonstrates that predicting the effect of increasing air temperatures on lake temperature by discontinuously modeling individual years based on the assumption that the temperature distribution in March is unaffected by climatic warming may be misleading and is certainly not justified in the case of Lake Zurich. Based on the continuous simulation, the temperature profile in Lake Zurich in March is influenced significantly by the heat accumulated during the previous year.

The main differences between our model results and earlier findings for other lakes can be explained by the fact that Lake Zurich does not freeze annually and that its winter surface temperatures are usually close to 4°C. In addition, because of the large depth of the lake, a significant amount of heat is stored in the hypolimnion and can accumulate from year to year. Modeling the thermal stratification in Lake Zurich therefore requires a continuous simulation, while in shallower lakes with annual ice cover a discontinuous simulation of the thermal structure of individual years with prescribed initial temperatures suffices. Note, however, that a discontinuous simulation will not suffice for lakes that are ice-covered during cold winters but not during warmer winters. In such cases, the ice cover present during cold winters insulates the bulk of the water body from further cooling, whereas the lack of ice cover during warmer winters can allow the water body to cool below 4°C (Livingstone 1993; Doran et al. 1996), appreciably influencing heat carryover.

References

BROCK, T. D. 1981. Calculating solar radiation for ecological studies. Ecol. Model. **14:** 1–19.

BURCHARD, H., AND H. BAUMERT. 1995. On the performance of a mixed-layer model based on the k-ε turbulence model. J. Geophys. Res. **100:** 8523–8540.

———, O. PETERSON, AND T. RIPPETH. 1998. Comparing the performance of the Mellor-Yamada and the k-ε two-equation turbulence models. J. Geophys. Res. **103:** 10543–10554.

DORAN, P. T., C. P. MCKAY, W. P. ADAMS, M. C. ENGLISH, R. A. WHARTON, JR., AND M. A. MEYER. 1996. Climate forcing and thermal feedback of residual lake-ice covers in the high Arctic. Limnol. Oceanogr. **41:** 839–848.

EDINGER, J. E., D. W. DUTTWEILER, AND J. C. GEYER. 1968. The response of water temperatures to meteorological conditions. Water Resour. Res. **4:** 1137–1143.

ELLIOTT, A. J. 1984. Measurements of the turbulence in an abyssal boundary layer. J. Phys. Oceanogr. **14:** 1778–1786.

ELO, A.-R., T. HUTTULA, A. PELTONEN, AND J. VIRTA. 1998. The effects of climate change on the temperature conditions of lakes. Boreal Environ. Res. **3:** 137–150.

FINCKH, P. 1981. Heat-flow measurements in 17 perialpine lakes: Summary. Geol. Soc. Am. Bull. **92:** 108–111.

GERTEN, D., AND R. ADRIAN. 2001. Differences in the persistency of the North Atlantic Oscillation signal among lakes. Limnol. Oceanogr. **46:** 448–455.

GILL, A. E. 1982. Atmosphere-ocean dynamics. Academic.

GLOOR, M., A. WÜEST, AND D. M. IMBODEN. 2000. Dynamics of

mixed bottom boundary layers and its implications for diapycnal transport in a stratified, natural water basin. J. Geophys. Res. **105:** 8629–8646.

GOUDSMIT, G.-H., H. BURCHARD, F. PEETERS, AND A. WÜEST. In press. Application of k-ε turbulence models to enclosed basins—the role of internal seiches. J. Geophys. Res.

HENDERSON-SELLERS, B. 1988. Sensitivity of thermal stratification models to changing boundary conditions. Appl. Math. Model. **12:** 31–43.

HOCKING, G. C. AND M. STRAŠKRABA. 1999. The effect of light extinction on thermal stratification in reservoirs and lakes. Internat. Rev. Hydrobiol. **84:** 535–556.

HONDZO, M., AND H. G. STEFAN. 1991. Three case studies of lake temperature and stratification response to warmer climate. Water Resour. Res. **27:** 1837–1846.

———, AND ———. 1992. Propagation of uncertainty due to variable meteorological forcing in lake temperature models. Water Resour. Res. **28:** 2629–2638.

———, AND ———. 1993. Regional water temperature characteristics of lakes subjected to climate change. Clim. Chang. **24:** 187–211.

HOSTETLER, S. W. 1995. Hydrological and thermal response of lakes to climate: Description and modeling, p. 63–82. *In* A. Lerman, D. M. Imboden, and J. Gatt [eds.], Physics and chemistry of lakes. Springer.

HOTTEL, H. C. 1976. A simple model for estimating the transmittance of direct solar radiation through clear atmosphere. Solar Energy **18:** 129–134.

HURRELL, J. W. 1995. Decadal trends in the North Atlantic Oscillation: Regional temperatures and precipitation. Science **269:** 676–679.

HUTTULA, T., A. PELTONEN, Ä. BILALETIN, AND M. SAURA. 1992. The effects of climatic change on lake ice and water temperature. Aqua Fenn. **22:** 129–142.

IMBODEN, D. M. 1990. Mixing and transport in lakes: Mechanisms and ecological relevance, p. 47–80. *In* M. Tilzer and C. Serruya, [eds.], Large lakes: Ecological structure and function. Springer.

———, AND A. WÜEST. 1995. Mixing mechanisms in lakes, p. 83–138. *In* A. Lerman, D. M. Imboden, and J. Gatt [eds.], Physics and chemistry of lakes. Springer.

KASTEN, F., AND G. CZEPLAK. 1980. Solar and terrestrial radiation dependent on the amount and type of cloud. Solar energy **24:** 177–189.

KATTENBERG, A., AND OTHERS. 1996. Climate models—Projection of future climate, p. 284–357. *In* J. T. Houghton, L. G. Meira Filho, B. A. Callander, N. Harris, A. Kattenberg, and K. Maskell [eds.], Climate change 1995—the science of climate change. Contribution of Working Group I to the Second Assessment Report of the Intergovernmental Panel on Climate Change. Cambridge Univ. Press.

KUHN, W. 1977. Berechnung der Temperatur und Verdunstung alpiner Seen auf klimatologisch-thermodynamischer Grundlage. Rep. 70, Swiss Meteorol. Inst.

———. 1978. Aus Wärmehaushalt und Klimadaten berechnete Verdunstung des Zürichsees. Vierteljahrsschr. Nat. forsch. Ges. Zürich **123:** 261–283.

KUTSCHKE, I. 1966. Die thermischen Verhältnisse im Zürichsee zwischen 1937 und 1963 und ihre Beeinflusssung durch meteorologische Faktoren. Vierteljahresschr. Nat. forsch. Ges. Zürich **111:** 47–124.

LEMANS, A. 1964. Die Seegefrörni 1963. Ann. Schweiz. Meteorol. Anst. **100 (Appendix 1):** 13–22.

LIVINGSTONE, D. M. 1993. Temporal structure in the deep-water temperature of four Swiss lakes: A short-term climatic change indicator? Verh. Int. Ver. Limnol. **25:** 75–81.

———. 1997. An example of the simultaneous occurrence of climate-driven ''sawtooth'' deep-water warming/cooling episodes in several Swiss lakes. Verh. Int. Ver. Limnol. **26:** 822–828.

———. In press. Impact of secular climate change on the thermal structure of a large temperate central European lake. Clim. Chang.

———, AND M. DOKULIL. 2001. Eighty years of spatially coherent Austrian lake surface temperatures and their relationship to regional air temperatures and the North Atlantic Oscillation. Limnol. Oceanogr. **46:** 1220–1227.

———, AND D. M. IMBODEN. 1989. Annual heat balance and equilibrium temperature of Lake Aegeri, Switzerland. Aquat. Sci. **51:** 351–369.

———, AND ———. 1996. The prediction of hypolimnetic oxygen profiles: A plea for a deductive approach. Can. J. Fish. Aquat. Sci. **53:** 924–932.

MOSES, T., G. N. KILADIS, H. F. DIAZ, AND R. G. BARRY. 1987. Characteristics and frequency of reversals in mean sea level pressure in the North Atlantic sector and their relationship to long-term temperature trends. J. Climatol. **7:** 13–30.

OMLIN, M., P. REICHERT, AND R. FORSTER. 2001. Biochemical model of Lake Zurich: Model equations and results. Ecol. Model. **144:** 77–103.

ÖRN, C. G. 1980. Die Sauerstoffverhältnisse im Zürichsee (Untersee) von 1937 bis 1975 und ihre Beeinflussung durch meteorologische Faktoren. Vierteljahrsschr. Nat. forsch. Ges. Zürich **125:** 259–364.

REYNOLDS, C. S. 1997. Vegetation processes in the pelagic: A model for ecosystem theory, p. 1–371. *In* O. Kinne [ed.], Excellence in ecology. Ecology Institute, Oldendorf.

ROBERTSON, D. M., AND R. A. RAGOTZKIE. 1990. Changes in the thermal structure of moderate to large sized lakes in response to changes in air temperature. Aquat. Sci. **52:** 360–380.

STEFAN, H. G., X. FANG, AND M. HONDZO. 1998. Simulated climate change effects on year-round water temperatures in temperate zone lakes. Clim. Chang. **40:** 547–576.

Received: 21 February 2001
Accepted: 29 August 2001
Amended: 4 October 2001